Molecular Therapy
Methods & Clinical Development
Original Article

Comparison of AAV-Mediated Optogenetic Vision Restoration between Retinal Ganglion Cell Expression and ON Bipolar Cell Targeting

Qi Lu,[1] Tushar H. Ganjawala,[1] Andrea Krstevski,[1] Gary W. Abrams,[1] and Zhuo-Hua Pan[1]

[1]Department of Ophthalmology, Visual and Anatomical Sciences, Wayne State University School of Medicine, Detroit, MI 48201, USA

The loss of photoreceptors in individuals with retinal degenerative diseases leads to partial or complete blindness. Optogenetic therapy is a promising approach for restoring vision to the blind. Multiple strategies have been employed by targeting genetically encoded light sensors, particularly channelrhodopsins, to surviving retinal neurons in animal models. In particular, the strategy of targeting retinal bipolar cells has commonly been expected to result in better vision than ubiquitous expression in retinal ganglion cells. However, a direct comparison of the channelrhodopsin-restored vision between these two strategies has not been performed. Here, we compared the restored visual functions achieved by adeno-associated virus (AAV)-mediated expression of a channelrhodopsin in ON-type bipolar cells and retinal ganglion cells driven by an improved mGluR6 promoter and a CAG promoter, respectively, in a blind mouse model by performing electrophysiological recordings and behavioral assessments. Unexpectedly, the efficacy of the restored vision based on light sensitivity and visual acuity was much higher following ubiquitous retinal ganglion cell expression than that of the strategy targeting ON-type bipolar cells. Our study suggests that, at least based on currently available gene delivery techniques, the expression of genetically encoded light sensors in retinal ganglion cells is likely a practical and advantageous strategy for optogenetic vision restoration.

INTRODUCTION

The severe loss of photoreceptor cells in individuals with inherited or acquired retinal degenerative diseases, such as retinitis pigmentosa (RP) and age-related macular degeneration (AMD), often leads to partial or complete blindness.[1,2] Currently, there is no effective treatment to restore vision to the blind, once photoreceptor cells have been lost. Optogenetics has emerged as a promising approach for restoring vision through the ectopic expression of genetically encoded light sensors (GELSs), particularly channelrhodopsins (ChRs), in surviving inner retinal neurons to impart light sensitivity to the retina.[3–8] This approach has the potential to treat all types of blindness caused by the death of photoreceptor cells, regardless of their underlying causes. It also has the potential to restore substantially high visual acuity because the restoration of retinal light sensitivity is achieved at the cellular level.

Multiple strategies have been employed to express GELSs in specific retinal cell types in animal models, primarily through adeno-associated virus (AAV)-mediated delivery. Most of the studies were based on the expression of GELSs in retinal ganglion cells (RGCs).[3,9–18] Others were based on targeting more distal retinal neurons, particularly ON-type bipolar cells (ON-BCs)[19–25] and even surviving cone photoreceptors.[26,27] The expression in RGCs is commonly achieved using ubiquitous promoters,[3,9,14,15] while the targeting of ON-BCs has mainly been achieved using mGluR6-based promoters.[19–23] Optogenetic therapy for the treatment of RP by AAV-mediated expression of ChRs driven by ubiquitous promoters in RGCs is currently in clinical trials (NCT02556736 and NCT03326336).

The strategy of targeting retinal BCs has commonly been considered to possess advantages over the ubiquitous expression in RGCs.[4–6,28] In mammalian retinas, the total number of BCs is approximately 10-fold higher than the number of RGCs.[29] The high density of BCs, together with the signal convergence from BCs to RGCs, is expected to improve light sensitivity and visual acuity. In addition, the targeting of BCs would partially preserve intrinsic visual processing in the retina, including the generation of ON and OFF light responses in RGCs that mimic their intrinsic light response polarity.[30,31] In contrast, the expression of GELS with a ubiquitous promoter in RGCs only converts them to all ON or all OFF cells.[3,12] Therefore, treatments targeting BCs are expected to result in better outcomes than ubiquitous expression in RGCs. Although the knowledge is important for the further development of effective optogenetic therapies, a direct, side-by-side comparison of the ChR restored visual functions between these two treatment strategies has not been performed.

In this study, we compared the restored visual functions between ubiquitous RGC expression and ON BC targeting through the AAV-mediated delivery of ChR by performing retinal

Received 15 May 2020; accepted 19 May 2020;
https://doi.org/10.1016/j.omtm.2020.05.009.

Correspondence: Zhuo-Hua Pan, PhD, Department of Ophthalmology, Visual and Anatomical Sciences, Wayne State University School of Medicine, 540 E. Canfield Avenue, Detroit, MI 48201, USA.
E-mail: zhpan@med.wayne.edu

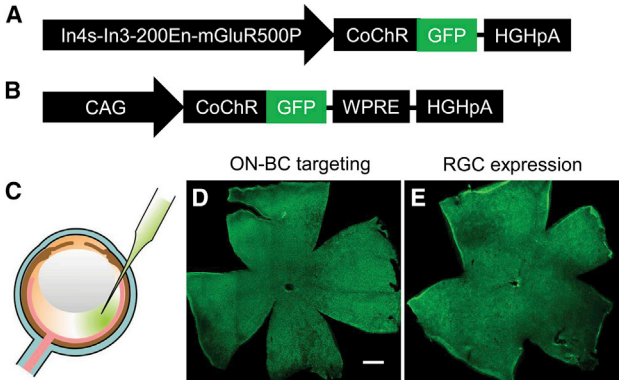

Figure 1. Virus Constructs and AAV-Mediated Expression of CoChR-GFP following ON-BC Targeting and Ubiquitous RGC Expression

(A and B) Schematic depicting the virus constructs used for ON-BC targeting with the mGluR6 promoter (A) and ubiquitous RGC expression with the CAG promoter (B). (C) Virus vectors were injected into the eye through an intravitreal injection. (D and E) Representative immunofluorescence images show a broad expression of CoChR-GFP over the entire retina viewed in retinal whole mounts following ON-BC targeting (D) and RGC expression (E). The images were captured from TKO mice. Scale bar, 500 μm.

electrophysiological recordings and behavioral tests. In particular, our study took advantage of using an improved ChR variant with increased light sensitivity,[18] and an improved mGluR6 promoter for the specific and efficient targeting of ON-BCs,[32] along with a blind $Opn4^{-/-}Gnat1^{-/-}Cnga3^{-/-}$ triple knockout (TKO) mouse model.[16] The TKO mice were chosen because they lack optomotor responses (OMRs), exhibit no pupillary constriction to light, and there is no apparent death of photoreceptor cells.[16,33,34] Together, these approaches facilitated the quantitative assessments of the restored visual functions by animal behavioral tests. Our results showed that the efficacy of the restored vision with RGC expression was much higher than that with BC-targeted ChR expression.

RESULTS

Comparison of Targeting Specificity and Transduction Efficiency of Virus Vectors

A highly light-sensitive ChR variant, CoChR-L112C,[18] fused to GFP (referred to as CoChR-GFP hereafter) was used in this study. The expression of CoChR-GFP in the retina was mediated by AAV vectors delivered through intravitreal administration (Figures 1A–1C). The targeted expression in ON-BCs (referred to as ON-BC targeting or BC targeting) was driven by an improved mGluR6 promoter, In4s-In3-200En-mGluR500P (Figure 1A).[32] The predominant expression in RGCs (referred to as RGC expression) was driven by a ubiquitous cytomegalovirus early enhancer/chicken β actin (CAG) promoter.[3] Broad expression over the entire retina was observed both in TKO mice (Figures 1D and 1E) and wild-type C57BL/6J mice (data not shown).

In mammalian retinas, BCs are classified into ON and OFF types. ON-BCs are composed of rod bipolar cells (RBCs) and ON-cone BCs (ON CBCs), whereas OFF-type BCs are all composed of OFF-cone bipolar cells (OFF-CBCs).[29,31] We first examined the targeting specificity and efficiency in BCs in TKO mice. For this purpose, BCs were labeled with anti-$G_{\gamma 13}$ and anti-protein kinase C (PKC) antibodies, the specific markers of all ON-BCs and RBCs, respectively.[35,36] As shown in retinal vertical sections with triple labeling (GFP/$G_{\gamma 13}$/PKC; Figures 2A–2F), the expression of GFP was mainly observed in ON-BCs in the inner nuclear layer, as evidenced by the co-labeling of GFP/$G_{\gamma 13}$ (Figure 2C). Additionally, the majority of RBCs were transduced, as evidenced by the co-labeling of GFP/PKC (Figure 2E). The specificity and transduction efficiency were quantitatively assessed in retinal whole mounts based on the triple labeling (Figures 2G–2L). As shown in the results of the statistical analysis presented in Table 1, ~72% of ON-BCs were transduced based on the co-labeling of GFP and $G_{\gamma 13}$, indicating a high transduction efficiency of the virus vectors to ON-BCs. Notably, ~85% of RBCs were transduced based on the co-labeling of GFP and PKC, while ~41% of ON-CBCs were transduced based on the number of GFP/$G_{\gamma 13}$ co-labeled but PKC-negative cells. Only ~16% of GFP-expressing BCs in the inner nuclear layer (INL) were $G_{\gamma 13}$-negative, indicating that the virus vectors were highly selective for ON-BCs.

As previously reported,[3,16,18] for the virus vectors containing the CAG promoter, GFP expression was observed in the vast majority of RGCs, many amacrine cells, and some horizontal cells (Figures S1A–S1C). On the other hand, GFP was rarely expressed in BCs. Based on the co-labeling of GFP with an anti-RBPMS antibody, a specific marker of RGCs, in retinal whole mounts, ~96% of RGCs were transduced by the virus vectors (Figures S1D–S1F; Table 1).

Comparison of CoChR-GFP Protein Expression by Western Blot Analysis

We next compared the CoChR-GFP protein expression in the whole retina between BC targeting and RGC expression by western blot analysis using an antibody against GFP. As shown in Figure 3, the relative band intensity of CoChR-GFP after normalized by the band intensity of β-actin in RGC expression (0.88 ± 0.07; mean ± SD; n = 3 retinas) is approximately 4 times as high as that in BC targeting (0.22 ± 0.01; mean ± SD; n = 3 retinas).

Comparison of CoChR-Mediated Light Sensitivity Using Multielectrode Array Recordings

We next examined the CoChR-mediated light response properties, particularly light sensitivity, of RGCs by performing multielectrode array (MEA) recordings from retinal whole mounts. The MEA recording method was chosen because a quantitative measurement can be made over a large number of cells and because the activities of RGCs represent the final outputs of the retina. Since photoreceptor-mediated light responses in TKO control mice were not detected under our light-adapted conditions,[18] most of the recordings in TKO mice were performed without pharmacological intervention for both BC targeting and RGC expression. Nevertheless, some recordings were performed in the presence of L-AP4 (20 μM) and ACET (2 μM) to block any potential synaptic inputs from

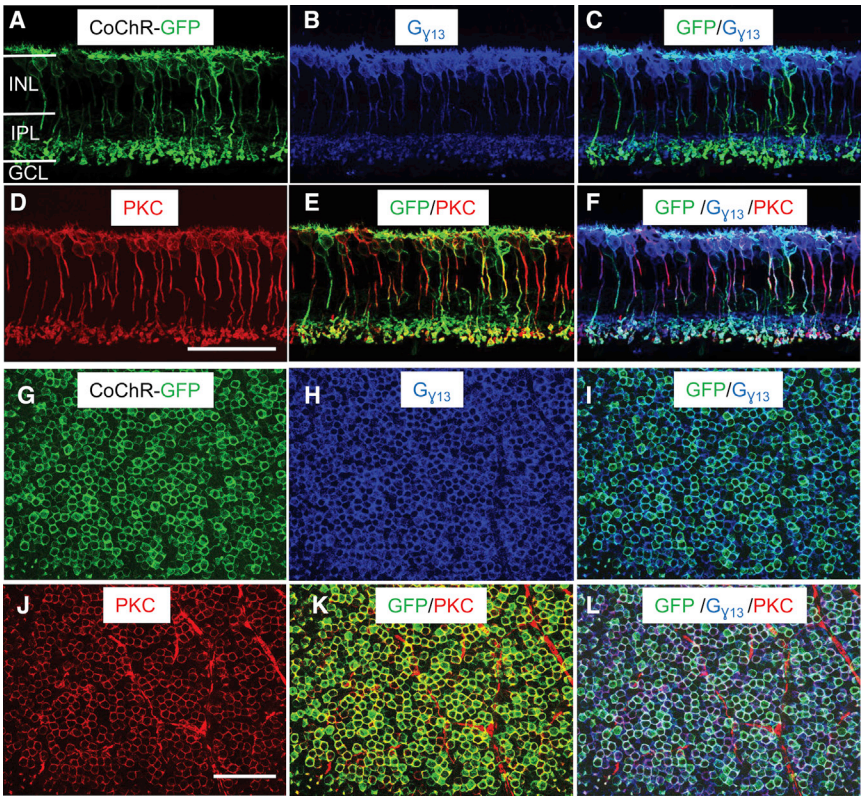

Figure 2. Expression and Specificity of CoChR-GFP following ON-BC Targeting

(A–L) Representative immunofluorescence images show the triple labeling of GFP (green), $G_{\gamma 13}$ (purple), and PKC (red) in retinal vertical sections (A–F) and retinal whole mounts (G–L). $G_{\gamma 13}$ and PKC are ON-BC- and RBC-specific markers, respectively. Images show single labeling of GFP (A and G), $G_{\gamma 13}$ (B and H), and PKC (D and J); double labeling of GFP/$G_{\gamma 13}$ (C and I) and GFP/PKC (E and K); and triple labelign of GFP/$G_{\gamma 13}$/PKC (F and L). As evidenced by the co-labeling of GFP/ $G_{\gamma 13}$ in retinal vertical sections, the expression of CoChR-GFP was almost exclusively targeted to ON-BCs in the inner nuclear layer (C). The majority of ON-BCs and RBCs were transduced by virus vectors based on the co-labeling of GFP/$G_{\gamma 13}$ (C and I) and GFP/PKC (E and K), respectively. The images of retinal whole mounts were captured with the focal plane in the inner nuclear layer. INL, inner nuclear layer; IPL, inner plexiform layer; GCL, ganglion cell layer. The images were captured from TKO mice. Scale bar, 50 μm.

photoreceptor cells with BC targeting, whereas other recordings were performed in the presence of a mixture of antagonists, i.e., CNQX (50 μM), D-AP5 (20 μM), L-AP4 (20 μM), ACET (2 μM), DHβE (20 μM), bicuculline (50 μM), and strychnine (5 μM), to block presynaptic inputs to RGCs with RGC expression. Recordings were also performed in C57BL/6J mice for both expressions, in which L-AP4 and ACET were used in all recordings, while the mixture of antagonists was used in some recordings with RGC expression. No significant differences were observed in the light sensitivity among TKO mice treated with and without the blockers or between TKO and C57BL/6J mice for both expressions and, therefore, the results were not differentiated.

The responses were elicited by 1 s light pulses at 480 nm with various light intensities adjusted by neutral density (ND) filters to compare the light sensitivity of CoChR-mediated spiking activities. The representative recordings obtained from mice subjected to BC targeting and RGC expression are shown in Figures 4A and 4B, respectively. Since the threshold light sensitivities varied among the recorded RGCs, the distribution curves for the normalized number of RGCs versus their threshold light sensitivity are shown in Figure 4C.

For the BC targeting, the lowest light intensity that elicited the spiking activities of RGCs was observed at ND 2.0 (~2.4×10^{14} photons/cm^2s; Figure 4A). This intensity was also the threshold light intensity that elicited the response of the highest number of RGCs (Figure 4C). The light response properties, however, were rather diverse. Both ON-OFF and ON light responses were observed (Figure 5). Among 194 recorded cells (3 retinas), 46% and 54% of the them showed ON-OFF and ON responses, respectively. The OFF response, when present, was blocked by strychnine (5 μM), a glycine receptor antagonist (the middle panel in Figure 5A), consistent with its origin in RBCs through glycinergic AII amacrine cells.[29] Furthermore, both the ON-OFF and ON light responses were mostly blocked by the addition of CNQX (50 μM), D-AP5 (20 μM), DHβE (20 μM), and bicuculline (50 μM; the bottom panel and lower panel in Figures 5A and 5B, respectively), except some small activities remained in a small portion of the cells (22 out of 114 cells; 2 retinas). The latter is likely due to the expression of a low level of CoChR due to off target effects. These results confirmed that the spiking activities recorded from RGCs primarily originated from CoChR-expressing BCs.

As previously reported,[18] the light responses observed with RGC expression were typically the sustained ON type, but they became more transient in response to higher light intensities (Figure 4B). The lowest light intensity that elicited the spiking activities of RGCs was 3.0 ND (~2.0×10^{13} photons/cm^2s; Figures 4B and 4C). This value was approximately 1 log unit lower than the values with BC targeting. The threshold light intensity that elicited the peak number of RGCs was 2.5 ND (~6.6×10^{13} photons/cm^2s; Figure 4C). The distribution curve of the number of RGCs versus the threshold light sensitivity following RGC expression was shifted approximately 0.5 log unit toward a lower light intensity than following BC targeting (Figure 4C). Together, RGC expression exhibits a much higher light sensitivity than BC targeting.

Table 1. Specificity and Efficiency of AAV-Mediated Retinal Cell Targeting

Cell Types	Labeling Antibodies	Cell Densities Number/mm^2	% of Targeting or Off-Targeting by ChR-GFP	Number of Retinas
ON-BCs	$G_{\gamma13}^+$	27,796 ± 2,866	72	3
	GFP$^+$/$G_{\gamma13}^+$	19,905 ± 3,275		
RBCs	PKC$^+$	19,341 ± 2,924	85	3
	GFP$^+$/PKC$^+$	16,439 ± 2,990		
ON-CBCs	$G_{\gamma13}^+$/PKC$^-$	8,455 ± 2,761	41	3
	GFP$^+$/$G_{\gamma13}^+$/PKC$^-$	3,466 ± 472		
Non ON-BCs	GFP$^+$	23,719 ± 2,260	16	3
	GFP$^+$/$G_{\gamma13}^-$	3,814 ± 2,495		
RGCs	RBPMS$^+$	3,700 ± 384	96	4
	GFP$^+$/RBPMS$^+$	3,549 ± 591		

The data are presented as the means ± SD.

Comparison of the Efficacy in Restoring Pupil Constriction

TKO mice lack the pupillary light reflex and their pupils are wide open, but pupil constriction can be partially restored by the expression of ChRs in RGCs.[16,33] Therefore, we next compared the efficacy of the restoration of pupil constriction in TKO mice. Pupil constriction was examined at the light intensity of 3×10^{15} photons/cm^{2}s. Marked pupil constriction (with a >50% reduction in the pupil area) was observed in 7 of 15 mice with RGC expression (Figure 6A). In contrast, the pupil constriction was not observed in any of the mice subjected to BC targeting (Figure 6B). The average percentage of the normalized pupil area in response to light stimulation following BC targeting (78% ± 5.9%; mean ± SD; n = 17) was significantly larger than following RGC expression (58% ± 20%; n = 15; one-way ANOVA, $p < 0.001$), but this value following BC targeting is not significantly different from the untreated control TKO mice (84% ± 3.3%; n = 11) (Figure 6C). Thus, RGC expression results in higher efficacy at restoring pupil constriction in TKO mice than BC targeting.

Comparison of the Efficacy of the Restoration of Optomotor Responses

TKO mice also lack OMRs, but OMRs can also be restored by the expression of ChRs in RGCs.[16,18,34] The OMR has been a commonly used assay for quantitatively assessing visual functions, including visual acuity.[37] Therefore, we further compared the efficacy of restoring OMR in TKO mice. The OMR was performed using a homemade optomotor testing system (Figure 7A).[16] Similar to RGC expression, a restoration of the OMR was also observed in the TKO mice with BC targeting. In both cases, the ability to elicit OMRs depended on the light intensity and grating frequency, with the most light-sensitive grating frequency at ~0.042 cycles/degree (Figure 7B). However, the average threshold light intensity required to elicit the OMR following BC targeting was 3.3×10^{14} photons/cm^{2}s (n = 10), a value that is approximately 1 log unit higher than the value observed after RGC expression (3.6×10^{13} photons/cm^{2}s; n = 8). Overall, the light intensity and spatial frequency curve observed with BC targeting was markedly shifted upward in comparison to the curve with RGC expression. Therefore, RGC expression results in higher visual acuity than BC targeting when compared at the same level of light intensity.

DISCUSSION

It has been commonly expected that BC targeting is a better treatment strategy than ubiquitous RGC expression for optogenetic vision restoration.[4–6,28] However, to our surprise, in this study, the outcome of the restored vision with RGC expression were much better than the outcomes observed with BC targeting. This conclusion is based on the results of three sets of experiments. First, in *ex vivo* retinal MEA recordings, the threshold light intensity required to elicit spike activities from RGCs following RGC expression was approximately 1 log unit lower than after BC targeting. Second, significant pupil constriction was observed in the treated TKO mice with RGC expression but not with BC targeting. Third, the threshold light intensity required to elicit the OMR in TKO mice with RGC expression was also approximately 1 log unit lower than BC targeting, while the restored visual acuity was markedly higher with RGC expression than with BC targeting.

It is worth noting that, following BC targeting, significant pupillary constriction was not observed even at the light intensity of 3×10^{15} photons/cm^{2}s whereas OMR was elicited at the light intensity of 3.3×10^{14} photons/cm^{2}s. This is because the threshold light intensity required to elicit OMR is lower than that required to evoke pupil constriction as we previously reported.[16]

In the present study, the experiments used to compare the outcomes between the two treatment strategies were performed under the same conditions, with the exception of the difference of the promoters and regulatory components and the total number of virus vectors injected. The number of injected virus particles for BC targeting was double the number applied for RGC expression to increase the expression of ChR in the BC targeting (see the Materials and Methods). Under our conditions, the majority (72%) of the ON-BCs were transduced. Therefore, the markedly lower light sensitivity and efficacy in BC targeting than in RGC expression could not be explained by the lack of targeting specificity or a low number of transduced ON-BCs.

Furthermore, unlike most previous studies examining BC targeting that were conducted using mouse models of retinal degeneration (*rd*),[19–25] the current study was performed in TKO mice. One of the advantages of using the TKO mouse model is the lack of apparent death of photoreceptor cells and thus likely avoiding substantial retinal remodeling.[16] Therefore, although retinal remodeling triggered by photoreceptor cell death is more severe to distal retinal neurons,[38–40] a significant contribution of retinal remodeling to the outcomes of BC targeting observed in this study is unlikely.

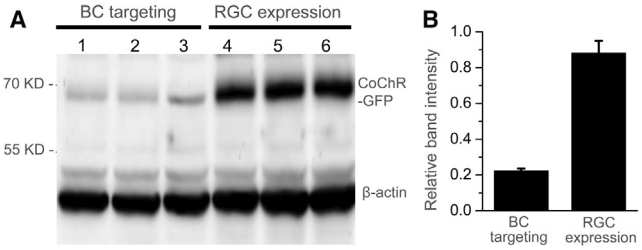

Figure 3. Comparison of CoChR-GFP Protein Expression between BC Targeting and RGC Expression by Western Blot Assay

(A) Western blot of CoChR-GFP protein levels from the whole retina with BC targeting (lines 1–3) and RGC expression (lines 4–6) using an antibody against GFP. The protein expression level of β-actin was served as control. (B) The relative band intensity of CoChR-GFP after normalized by the band intensity of β-actin in RGC expression (0.88 ± 0.07; mean ± SD; n = 3 retinas) and in BC targeting (0.22 ± 0.01; mean ± SD; n = 3 retinas).

The high density of BCs and the convergence from BCs to RGCs is expected to improve light sensitivity and visual acuity with BC targeting. What are the potential causes of the worse outcomes in BC targeting than in RGC expression? Several possible factors or mechanisms could affect the light sensitivity in particular. First, the expression in BCs was driven by the mGluR6 promoter,[32,41] an endogenous promoter, whereas expression in RGCs was driven by the CAG promoter, a strong viral promoter.[42] Although a much improved mGluR6 promoter was used in this study,[32] endogenous promoters are generally weaker than viral promoters. In addition, the efficiency of virus delivery to BCs is likely to be lower than RGCs due to the physical barriers that the virus particles must penetrate to enter the middle retinal layer following intravitreal injection.[43] Together, the ChR expression in BCs is expected to be lower than RGCs, contributing to its lower light sensitivity. Indeed, our western blot results showed that ChR-GFP protein level in the retina with RGC expression was 3 times higher than BC targeting. Although the expression of ChR-GFP in amacrine cells and horizontal cells in part contributed to the higher protein level in RGC expression, the ChR-GFP expression in RGCs is likely still substantially higher than in BCs. Second, since the ChR in RGCs is expressed throughout the entire membrane, the ChR-mediated current produced over the large membrane of an RGC may be more effective at eliciting spiking than the glutamate receptor-mediated current at the postsynaptic sites of its distal dendrites, thus resulting in greater light sensitivity. In addition, other factors, such as a suppression of BC to RGC synaptic transmission following the expression of ChR in BCs, cannot be excluded.

Since the light sensitivity of ChRs is critically correlated with the restored visual functions,[16,18] the low light sensitivity in BC targeting is likely to partially contribute to its low functional efficacy.

Further studies are needed to investigate the major factors causing the low light sensitivity and efficacy in BC targeting. Experiments using a ChR reporter mouse line combining ON-BC- and RGC-specific Cre mouse lines could be performed to achieve equal ChR expression between ON-BCs and RGCs.[44,45] The studies could determine whether or to what extent ChR expression contributes to the light sensitivity and functional efficacy. Accordingly, efforts may be directed to further improve transgene expression, including promotor strength for BC targeting. Since AAV-mediated gene delivery has been the most powerful method for retinal gene therapy,[46,47] any limitation related to the virus-mediated delivery, including promoter strength,[32,43] needs to be considered when evaluating the effectiveness of optogenetic treatment strategies. Furthermore, the impact of retinal modeling after photoreceptor degeneration on the targeting specificity, delivery efficiency, and functional outcomes will also need to be taken into consideration in future studies.[38,48]

Another major advantage of targeting BCs is the potential restoration of intrinsic visual processing in the retina, including intrinsic ON and OFF light responses. Consistent with previous reports,[19,21,22] the use of a strategy targeting ON-BCs indeed produced both ON and OFF light responses in RGCs in the present study. However, our results suggest that this potential advantage of the restoration of intrinsic visual processing was offset by its other drawbacks based on the assessment methods carried by the current study. Whether there are advantages for BC targeting to restore more complex visual function remains to be investigated.

On the other hand, advantages of RGC expression include the accessibility of viral delivery through intravitreal injection and are likely less affected by retinal remodeling.[43,49] A major question raised regarding the ubiquitous RGC expression concerns whether the unnatural visual signals can result in useful vision.[50] To date, the ability of this strategy to restore functional vision has been extensively validated in animal models.[9–11,13–18] All the current ongoing clinical trials for optogenetic vision restoration are being conducted by ubiquitous RGC expression. Furthermore, the restoration of remarkably good visual acuity and/or contrast sensitivity following ubiquitous RGC expression has been recently reported in mouse models,[17,18] suggesting the substantial ability of the brain to adapt new visual signals. It should be noted that, as the RGC expression was achieved by using ubiquitous CAG promoter in this study, the expression was also observed in many amacrine cells and some horizontal cells. The contribution of ChR-expressing amacrine cells and horizontal cells to the restored visual functions remains to be investigated. Therefore, further studies would be interesting to investigate whether targeting specific populations or subcellular compartments of RGCs by using versatile GELSs to create ON and OFF responses or center-surround receptive fields at the level of RGCs can improve the restored visual functions.[12,51,52]

Taken together, our study suggests that, at least based on currently available techniques, RGC expression driven by ubiquitous promoters is likely a practical and advantageous strategy for optogenetic vision restoration.

MATERIALS AND METHODS

Animals and AAV Vectors

A TKO, Opn4$^{-/-}$ Gnat1$^{-/-}$ Cnga3$^{-/-}$, blind mouse line was used.[16,33] The expression analyses and physiological recordings were also

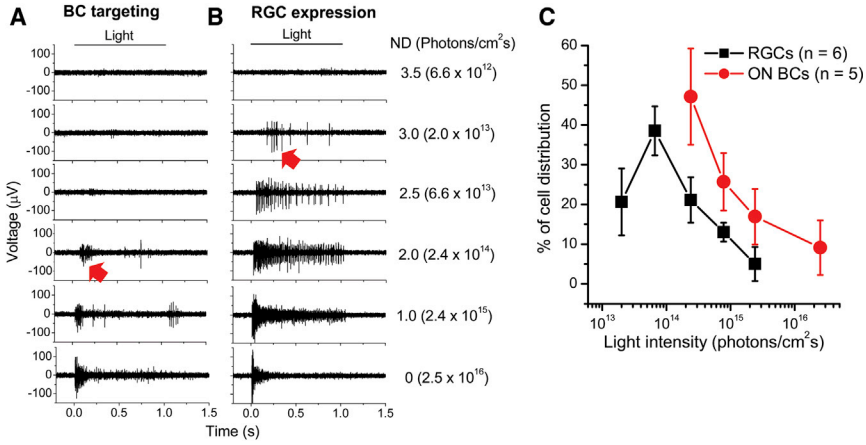

Figure 4. Comparison of the Light Sensitivity of CoChR-Mediated Light Responses between BC Targeting and RGC Expression Using Multielectrode Array Recordings

(A and B) Representative recordings of CoChR-mediated spiking activities with BC targeting (A) and RGC expression (B) in TKO mice. The spiking activities were elicited by 1 s light pulses with incrementally increasing light intensities adjusted with neutral density (ND) filters of 3.5, 3.0, 2.5, 2.0, 1.0, and 0. The light intensities measured as photons/cm^{2}s are also shown. The threshold light intensities required to elicit spiking activities following BC targeting and RGC expression were observed with ND filters of 2.0 and 3.0, respectively (marked with arrows). (C) Comparison of the distribution of the normalized number of RGCs (average from the recorded retinas) versus threshold light intensities between BC targeting (mean ± SD; 5 retinas; 257 cells) and RGC expression. The data for RGC expression (6 retinas; 299 cells) were adapted from our previously published paper.[18]

performed in normal C57BL/6J mice. All animal experiments and procedures were approved by the Institutional Animal Care and Use Committee of Wayne State University and were performed in accordance with the NIH Guide for the Care and Use of Laboratory Animals.

Virus vectors were packaged in the AAV2.7m8-Y444F capsid variant,[32,53,54] and affinity purified by Virovek (Hayward, CA, USA). Virus vectors were injected as described previously.[16] Briefly, animals aged at least 1 month were anesthetized with an intraperitoneal injection of a mixture of 100 mg/kg^{-1} ketamine and 12 mg/kg^{-1} xylazine. Virus vectors of 1.5 μL at a titer of 5×10^{12} vg/mL with CAG promoter and 1×10^{13} vg/mL with mGluR6 promoter were intravitreally injected into both eyes of each animal. The injection was made through glass micropipettes using a programmable Nanoliter Injector (Drummond Scientific Company, Broomall, PA, USA). All experiments were performed at least 1 month after virus injection. Animals

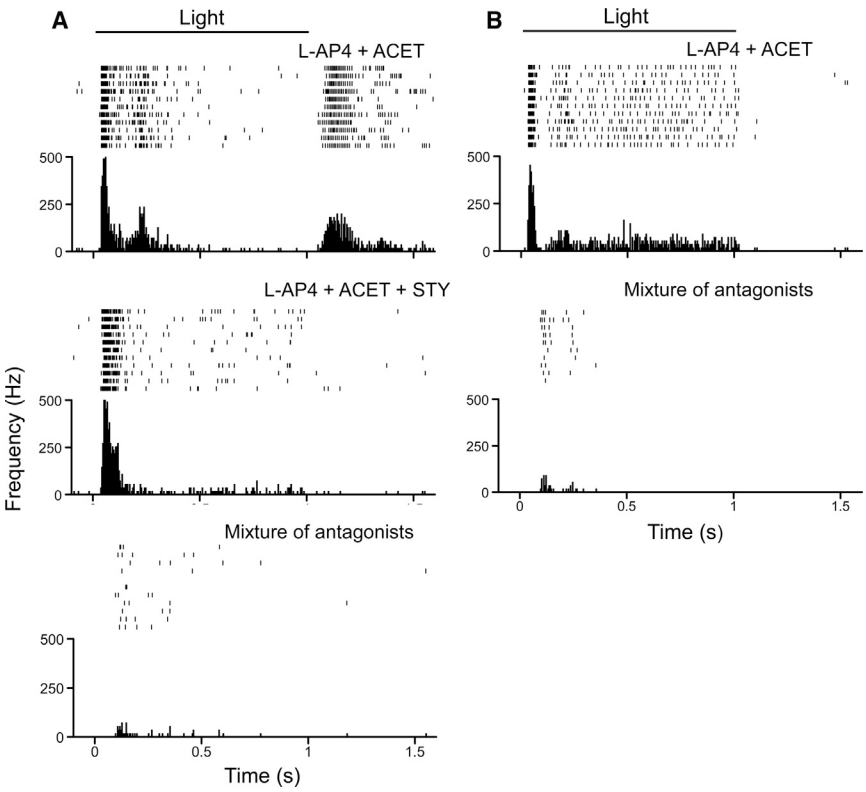

Figure 5. Properties of CoChR-Mediated Light Responses following BC Targeting in Multielectrode Recordings

(A) Representative recordings of CoChR-mediated spiking activities exhibiting ON and OFF light responses in the presence of L-AP4 (20 μM) and ACET (2 μM) (top panel). The OFF response was blocked by the addition of strychnine (5 μM; middle panel). The ON response was further blocked by the addition of a mixture of CNQX (50 μM), D-AP5 (20 μM), DHβE (20 μM), and bicuculline (50 μM; bottom panel). (B) Representative recordings of CoChR-mediated spiking activities showing ON light responses in the presence of L-AP4 and ACET. The ON response was mostly blocked by the mixture of antagonists (lower panel). The spiking activities were elicited by 1 s light pulses at 480 nm with the light intensity of 2.4×10^{15} photons/cm^{2}s. In each panel, a raster plot of 10 consecutive recordings, and an averaged spike rate histogram are shown in the top and bottom panels, respectively. The recordings were made from TKO mice.

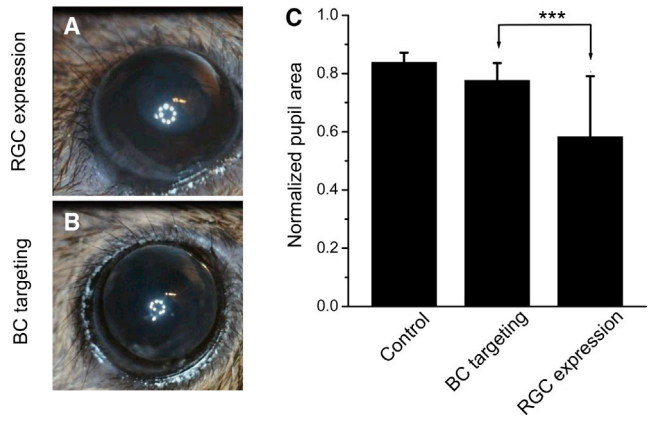

Figure 6. Comparison of the CoChR-Mediated Pupillary Constriction in TKO Mice between BC Targeting and RGC Expression

(A and B) Representative images of TKO mice expressing CoChR after BC targeting and RGC expression in response to light stimulation. Marked pupil constriction was observed in mice with RGC expression (A), but not in mice with BC targeting (B). (C) The average percentage of the normalized pupil area in response to light stimulation with BC targeting (78% ± 5.9%; mean ± SD; n = 17) is significantly different from RGC expression (58% ± 20%; n = 15; one-way ANOVA, $p < 0.001$) but is not significantly different from the untreated control mice (84% ± 3.3%; n = 11). Light intensity: 3×10^{15} photons/cm^{2}s with blue LED illumination (470 nm).

were euthanized by CO_2 asphyxiation followed by decapitation for electrophysiological recordings and immunostaining.

Immunostaining and Cell Density Measurements

Enucleated eyes were fixed with 4% paraformaldehyde in phosphate buffer (PB) at room temperature for 20 min. Immunofluorescence staining was examined in retinal vertical sections and retinal whole mounts. The following primary antibodies were used in this study: mouse anti-GFP (1:1000; Neuromab, UC Davis, Davis, CA, USA), mouse anti-PKC (1:10,000; Santa Cruz, Dallas, TX, USA), rabbit anti-$G_{\gamma 13}$ (1:1,000; sc-368324, Santa Cruz, Dallas, TX, USA), and rabbit anti-RBPMS (1:1,000; ABN1362, MilliporeSigma, Temecula, CA, USA). The secondary antibodies were conjugated to Alexa 488 (1:600), Alexa 555 (1:1,000), or Alexa 594 (1:500; Thermo Fisher Scientific, Waltham, MA, USA). Fluorescence images were obtained using a ZEISS APOTOME2 Optical Photomicroscope (Apotome; Carl Zeiss Microscopy GmbH, Jena, Germany).

For counting cell densities, images of 10–15 planes in the ganglion cell layer at an interval of 1 μm and 25–35 planes in the inner nuclear layer at an interval of 0.5 μm were captured for RGC expression and BC targeting, respectively, in retinal whole mounts. Three to eight images were captured in the middle regions of each retina (~1–1.5 mm from the optic disc). The brightness and the contrast were adjusted using the ZEN2 software. RGC counting was performed using stacked images generated in ZEN2-3D mode. BC counting was performed from one of every five planes (or at an interval of 2.5 μm) to ensure the cells were not counted repeatedly. The total BC numbers were the sum of all the chosen planes.

Western Blot Analysis

Retinal tissue was lysed by sonication in radioimmunoprecipitation assay (RIPA) buffer (89901 Pierce, Thermo Fisher Scientific) with a 1% protease inhibitor cocktail (P8340; Sigma-Aldrich, St. Louis, MO, USA) and followed by centrifugation. After quantification of total protein with Pierce BCA Protein Assay Kit (23225, Thermo Fisher Scientific), the protein lysates were adjusted to 1 μg/μL, mixed with 2× Laemmli sample buffer (S3401, Sigma-Aldrich), and boiled for 10 min. Total protein samples (40 μg) were run on a 10% SDS-PAGE in Tris glycine-SDS buffer (LC2675, Thermo Fisher Scientific) for 1 h at 100V. Then the proteins were transferred to a nitrocellulose membrane at 4°C for 2 h. After blocking with 5% Chemiblocker (MilliporeSigma) in 1× Tris-buffered saline containing 0.1% Tween 20 (TBS-T) for 1 h in 4°C, the membrane was immunostained with the rabbit anti-GFP primary antibody (1:1,000; A11122, Life Technologies, CA, USA) and rabbit anti-β-actin primary antibody (1:1,000; PA5-72633, Life Technologies) in TBS-T overnight at 4°C. The membrane was washed with 1× TBST three times and then incubated with a goat anti-rabbit horseradish peroxidase secondary antibody (1:2,000, W4011, Promega, Madison, WI, USA) diluted in TBS-T with 5% Chemiblocker at room temperature for 2 h. Bands were visualized and analyzed using a FluorChem System (Proteinsimple, San Jose, CA, USA). The intensity of the band was analyzed with AlphaView software installed in the FluorChem system for semi-quantification.

MEA Recordings

MEA recordings were performed using previously described procedures.[3,18] Briefly, the mounted retina was placed in the MEA-60 recording chamber (Multi Channel System MCS GmbH, Reutlingen, Germany). The retina was continuously perfused with an oxygenated extracellular solution at 34°C during all experiments. The extracellular solution contained (in mM): 124 NaCl, 2.5 KCl, 2 $CaCl_2$, 2 $MgCl_2$, 1.25 NaH_2PO_4, 26 $NaHCO_3$, and 22 glucose, pH 7.35 with 95% O_2 and 5% CO_2. The following antagonists were used: 6-cyano-7-nitroquinoxaline-2,3-dione (CNQX; 50 μM), D(−)-2-amino-5-phosphonopentanoic acid (D-AP5; 20 μM), L-(+)-2-amino-4-phosphonobutyric acid (L-AP4; 20 μM), ACET (2 μM), dihydro-β-erythroidine (DHβE; 20 μM), bicuculline (50 μM), and strychnine (5 μM). The interval between the onset of each light stimulus was 20 s. Spike sorting was performed for classifying ON and OFF cells, but not for determining threshold light sensitivity. For the latter, one cell with the lowest threshold in each recording electrode was counted. Signals were filtered between 200 Hz (low cutoff) and 20 kHz (high cutoff). A threshold of 24 μV was used to detect action potentials. For spike sorting, action potentials from individual neurons were determined with a standard expectation-maximization algorithm using offline Sorter software (Plexon, Dallas, TX, USA). The raster plots and average spike rate histograms were plotted using NeuroExplorer software (Nex Technologies, Madison, AL, USA). Light stimuli were generated by 150 W xenon lamp-based scanning monochromators with a bandwidth of 10 nm (TILL Photonics, Germany). The light stimuli were directly projected onto the bottom of the recording chamber through an optical fiber. The light intensity was attenuated by ND filters.

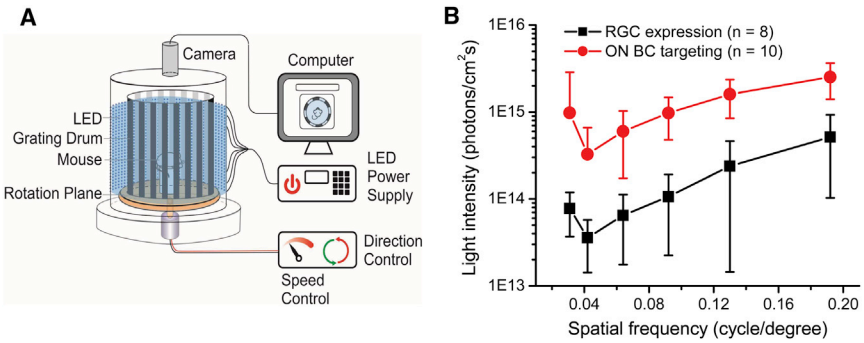

Figure 7. Comparison of the Efficacies of the Restoration of the OMR in CoChR-Treated TKO Mice between BC Targeting and RGC Expression

(A) A schematic depicting the homemade optomotor system using blue (470 nm) LEDs as the light illumination source. (B) The spatial frequency-dependent threshold light intensity curves for mice with BC targeting (n = 10) and RGC expression (n = 8). All data are presented as the means ± SD from the indicated number of animals.

Measurement of Pupillary Constriction

During measurements, animals were restrained by hand under a blue LED with a peak wavelength of 470 nm. The light intensity was 3×10^{15} photons/cm^{2}s, measured at the site of the mouse eyes. The direct pupillary reflex to light was measured in one eye of each animal. Multiple images and videos were acquired within 10 s span using a digital camera before and during the light stimulation to measure the normalized pupil area.

Optomotor Response Experiment

Optomotor responses were examined using a homemade optomotor system as previously described.[16] Light illumination was provided by blue (470 nm) LEDs. Head tracking was tested in both clockwise and counterclockwise directions. The threshold light intensity at each grating frequency required to evoke the OMR was determined. Data obtained from the two directions of drum rotation for each animal were treated as two independent data points in the analysis. The experimental data were confirmed by a second experimenter.

SUPPLEMENTAL INFORMATION

Supplemental Information can be found online at https://doi.org/10.1016/j.omtm.2020.05.009.

AUTHOR CONTRIBUTIONS

Q.L., G.W.A., and Z.-H.P. designed the experiments. Q.L., T.H.G., A.K., and Z.-H.P. performed experiments and analyzed data; Q.L. and Z.-H.P. wrote and G.W.A. edited the paper.

CONFLICTS OF INTEREST

Z.-H.P., Q.L., T.H.G., and G.W.A. are inventors on patents and patent applications related to optogenetic vision restoration. Z.-H.P. and G.W.A. previously served as consultants to RetroSense Therapeutics company. A.K. declares no competing interests.

ACKNOWLEDGMENTS

This work was supported by the Ligon Research Center of Vision at Kresge Eye Institute, Dryer Foundation, Herrick Foundation, an unrestricted grant to the Department of Ophthalmology, Visual and Anatomical Sciences by Research to Prevent Blindness Inc., United States, and NIH, United States, core grant EY04068 to Department of Ophthalmology, Visual and Anatomical Sciences at Wayne State University School of Medicine. We thank Mitchell Fenner and Anna Wright for technical assistance.

REFERENCES

1. Hartong, D.T., Berson, E.L., and Dryja, T.P. (2006). Retinitis pigmentosa. Lancet *368*, 1795–1809.
2. de Jong, P.T. (2006). Age-related macular degeneration. N. Engl. J. Med. *355*, 1474–1485.
3. Bi, A., Cui, J., Ma, Y.P., Olshevskaya, E., Pu, M., Dizhoor, A.M., and Pan, Z.H. (2006). Ectopic expression of a microbial-type rhodopsin restores visual responses in mice with photoreceptor degeneration. Neuron *50*, 23–33.
4. Busskamp, V., Picaud, S., Sahel, J.A., and Roska, B. (2012). Optogenetic therapy for retinitis pigmentosa. Gene Ther. *19*, 169–175.
5. Barrett, J.M., Berlinguer-Palmini, R., and Degenaar, P. (2014). Optogenetic approaches to retinal prosthesis. Vis. Neurosci. *31*, 345–354.
6. Pan, Z.-H., Lu, Q., Bi, A., Dizhoor, A.M., and Abrams, G.W. (2015). Optogenetic approaches to restoring vision. Annu. Rev. Vis. Sci. *1*, 185–210.
7. Baker, C.K., and Flannery, J.G. (2018). Innovative optogenetic strategies for vision restoration. Front. Cell. Neurosci. *12*, 316.
8. Simunovic, M.P., Shen, W., Lin, J.Y., Protti, D.A., Lisowski, L., and Gillies, M.C. (2019). Optogenetic approaches to vision restoration. Exp. Eye Res. *178*, 15–26.
9. Tomita, H., Sugano, E., Yawo, H., Ishizuka, T., Isago, H., Narikawa, S., Kügler, S., and Tamai, M. (2007). Restoration of visual response in aged dystrophic RCS rats using AAV-mediated channelopsin-2 gene transfer. Invest. Ophthalmol. Vis. Sci. *48*, 3821–3826.
10. Tomita, H., Sugano, E., Murayama, N., Ozaki, T., Nishiyama, F., Tabata, K., Takahashi, M., Saito, T., and Tamai, M. (2014). Restoration of the majority of the visual spectrum by using modified Volvox channelrhodopsin-1. Mol. Ther. *22*, 1434–1440.
11. Lin, B., Koizumi, A., Tanaka, N., Panda, S., and Masland, R.H. (2008). Restoration of visual function in retinal degeneration mice by ectopic expression of melanopsin. Proc. Natl. Acad. Sci. USA *105*, 16009–16014.
12. Zhang, Y., Ivanova, E., Bi, A., and Pan, Z.-H. (2009). Ectopic expression of multiple microbial rhodopsins restores ON and OFF light responses in retinas with photoreceptor degeneration. J. Neurosci. *29*, 9186–9196.
13. Nirenberg, S., and Pandarinath, C. (2012). Retinal prosthetic strategy with the capacity to restore normal vision. Proc. Natl. Acad. Sci. USA *109*, 15012–15017.
14. Sengupta, A., Chaffiol, A., Macé, E., Caplette, R., Desrosiers, M., Lampič, M., Forster, V., Marre, O., Lin, J.Y., Sahel, J.A., et al. (2016). Red-shifted channelrhodopsin stimulation restores light responses in blind mice, macaque retina, and human retina. EMBO Mol. Med. *8*, 1248–1264.
15. Chaffiol, A., Caplette, R., Jaillard, C., Brazhnikova, E., Desrosiers, M., Dubus, E., Duhamel, L., Macé, E., Marre, O., Benoit, P., et al. (2017). A new promoter allows

optogenetic vision restoration with enhanced sensitivity in macaque retina. Mol. Ther. *25*, 2546–2560.

16. Lu, Q., Ganjawala, T.H., Hattar, S., Abrams, G.W., and Pan, Z.-H. (2018). A Robust optomotor assay for assessing the efficacy of optogenetic tools for vision restoration. Invest. Ophthalmol. Vis. Sci. *59*, 1288–1294.
17. Berry, M.H., Holt, A., Salari, A., Veit, J., Visel, M., Levitz, J., Aghi, K., Gaub, B.M., Sivyer, B., Flannery, J.G., and Isacoff, E.Y. (2019). Restoration of high-sensitivity and adapting vision with a cone opsin. Nat. Commun. *10*, 1221.
18. Ganjawala, T.H., Lu, Q., Fenner, M.D., Abrams, G.W., and Pan, Z.-H. (2019). Improved CoChR variants restore visual acuity and contrast sensitivity in a mouse model of blindness under ambient light conditions. Mol. Ther. *27*, 1195–1205.
19. Lagali, P.S., Balya, D., Awatramani, G.B., Münch, T.A., Kim, D.S., Busskamp, V., Cepko, C.L., and Roska, B. (2008). Light-activated channels targeted to ON bipolar cells restore visual function in retinal degeneration. Nat. Neurosci. *11*, 667–675.
20. Doroudchi, M.M., Greenberg, K.P., Liu, J., Silka, K.A., Boyden, E.S., Lockridge, J.A., Arman, A.C., Janani, R., Boye, S.E., Boye, S.L., et al. (2011). Virally delivered channelrhodopsin-2 safely and effectively restores visual function in multiple mouse models of blindness. Mol. Ther. *19*, 1220–1229.
21. Cronin, T., Vandenberghe, L.H., Hantz, P., Juttner, J., Reimann, A., Kacsó, A.E., Huckfeldt, R.M., Busskamp, V., Kohler, H., Lagali, P.S., et al. (2014). Efficient transduction and optogenetic stimulation of retinal bipolar cells by a synthetic adeno-associated virus capsid and promoter. EMBO Mol. Med. *6*, 1175–1190.
22. Macé, E., Caplette, R., Marre, O., Sengupta, A., Chaffiol, A., Barbe, P., Desrosiers, M., Bamberg, E., Sahel, J.A., Picaud, S., et al. (2015). Targeting channelrhodopsin-2 to ON-bipolar cells with vitreally administered AAV Restores ON and OFF visual responses in blind mice. Mol. Ther. *23*, 7–16.
23. van Wyk, M., Pielecka-Fortuna, J., Löwel, S., and Kleinlogel, S. (2015). Restoring the ON switch in blind retinas: Opto-mGluR6, a next-generation, cell-tailored opotogenetic tool. PLoS Biol. *13*, e1002143.
24. Gaub, B.M., Berry, M.H., Holt, A.E., Isacoff, E.Y., and Flannery, J.G. (2015). Optogenetic vision restoration using rhodopsin for enhanced sensitivity. Mol. Ther. *23*, 1562–1571.
25. Cehajic-Kapetanovic, J., Eleftheriou, C., Allen, A.E., Milosavljevic, N., Pienaar, A., Bedford, R., Davis, K.E., Bishop, P.N., and Lucas, R.J. (2015). Restoration of vision with ectopic expression of human rod opsin. Curr. Biol. *25*, 2111–2122.
26. Busskamp, V., Duebel, J., Balya, D., Fradot, M., Viney, T.J., Siegert, S., Groner, A.C., Cabuy, E., Forster, V., Seeliger, M., et al. (2010). Genetic reactivation of cone photoreceptors restores visual responses in retinitis pigmentosa. Science *329*, 413–417.
27. Garita-Hernandez, M., Lampič, M., Chaffiol, A., Guibbal, L., Routet, F., Santos-Ferreira, T., Gasparini, S., Borsch, O., Gagliardi, G., Reichman, S., et al. (2019). Restoration of visual function by transplantation of optogenetically engineered photoreceptors. Nat. Commun. *10*, 4524.
28. Klapper, S.D., Swiersy, A., Bamberg, E., and Busskamp, V. (2016). Biophysical properties of optogenetic tools and their application for vision restoration approaches. Front. Syst. Neurosci. *10*, 74.
29. Wässle, H., and Boycott, B.B. (1991). Functional architecture of the mammalian retina. Physiol. Rev. *71*, 447–480.
30. Bloomfield, S.A., and Dacheux, R.F. (2001). Rod vision: pathways and processing in the mammalian retina. Prog. Retin. Eye Res. *20*, 351–384.
31. Euler, T., Haverkamp, S., Schubert, T., and Baden, T. (2014). Retinal bipolar cells: elementary building blocks of vision. Nat. Rev. Neurosci. *15*, 507–519.
32. Lu, Q., Ganjawala, T.H., Ivanova, E., Cheng, J.G., Troilo, D., and Pan, Z.-H. (2016). AAV-mediated transduction and targeting of retinal bipolar cells with improved mGluR6 promoters in rodents and primates. Gene Ther. *23*, 680–689.
33. Hattar, S., Lucas, R.J., Mrosovsky, N., Thompson, S., Douglas, R.H., Hankins, M.W., Lem, J., Biel, M., Hofmann, F., Foster, R.G., and Yau, K.W. (2003). Melanopsin and rod-cone photoreceptive systems account for all major accessory visual functions in mice. Nature *424*, 76–81.
34. Ecker, J.L., Dumitrescu, O.N., Wong, K.Y., Alam, N.M., Chen, S.K., LeGates, T., Renna, J.M., Prusky, G.T., Berson, D.M., and Hattar, S. (2010). Melanopsin-expressing retinal ganglion-cell photoreceptors: cellular diversity and role in pattern vision. Neuron *67*, 49–60.
35. Huang, L., Max, M., Margolskee, R.F., Su, H., Masland, R.H., and Euler, T. (2003). G protein subunit G γ 13 is coexpressed with G α o, G β 3, and G β 4 in retinal ON bipolar cells. J. Comp. Neurol. *455*, 1–10.
36. Greferath, U., Grünert, U., and Wässle, H. (1990). Rod bipolar cells in the mammalian retina show protein kinase C-like immunoreactivity. J. Comp. Neurol. *301*, 433–442.
37. Prusky, G.T., Alam, N.M., Beekman, S., and Douglas, R.M. (2004). Rapid quantification of adult and developing mouse spatial vision using a virtual optomotor system. Invest. Ophthalmol. Vis. Sci. *45*, 4611–4616.
38. Marc, R.E., Jones, B.W., Watt, C.B., and Strettoi, E. (2003). Neural remodeling in retinal degeneration. Prog. Retin. Eye Res. *22*, 607–655.
39. Mazzoni, F., Novelli, E., and Strettoi, E. (2008). Retinal ganglion cells survive and maintain normal dendritic morphology in a mouse model of inherited photoreceptor degeneration. J. Neurosci. *28*, 14282–14292.
40. Damiani, D., Novelli, E., Mazzoni, F., and Strettoi, E. (2012). Undersized dendritic arborizations in retinal ganglion cells of the rd1 mutant mouse: a paradigm of early onset photoreceptor degeneration. J. Comp. Neurol. *520*, 1406–1423.
41. Kim, D.S., Matsuda, T., and Cepko, C.L. (2008). A core paired-type and POU homeodomain-containing transcription factor program drives retinal bipolar cell gene expression. J. Neurosci. *28*, 7748–7764.
42. Miyazaki, J., Takaki, S., Araki, K., Tashiro, F., Tominaga, A., Takatsu, K., and Yamamura, K. (1989). Expression vector system based on the chicken beta-actin promoter directs efficient production of interleukin-5. Gene *79*, 269–277.
43. Dalkara, D., Kolstad, K.D., Caporale, N., Visel, M., Klimczak, R.R., Schaffer, D.V., and Flannery, J.G. (2009). Inner limiting membrane barriers to AAV-mediated retinal transduction from the vitreous. Mol. Ther. *17*, 2096–2102.
44. Lu, Q., Ivanova, E., Ganjawala, T.H., and Pan, Z.-H. (2013). Cre-mediated recombination efficiency and transgene expression patterns of three retinal bipolar cell-expressing Cre transgenic mouse lines. Mol. Vis. *19*, 1310–1320.
45. Daigle, T.L., Madisen, L., Hage, T.A., Valley, M.T., Knoblich, U., Larsen, R.S., Takeno, M.M., Huang, L., Gu, H., Larsen, R., et al. (2018). A suite of transgenic driver and reporter mouse lines with enhanced brain-cell-type targeting and functionality. Cell *174*, 465–480.e22.
46. Surace, E.M., and Auricchio, A. (2008). Versatility of AAV vectors for retinal gene transfer. Vision Res. *48*, 353–359.
47. Vandenberghe, L.H., and Auricchio, A. (2012). Novel adeno-associated viral vectors for retinal gene therapy. Gene Ther. *19*, 162–168.
48. van Wyk, M., Hulliger, E.C., Girod, L., Ebneter, A., and Kleinlogel, S. (2017). Present molecular limitations of ON-bipolar cell targeted gene therapy. Front. Neurosci. *11*, 161.
49. Marc, R., Pfeiffer, R., and Jones, B. (2014). Retinal prosthetics, optogenetics, and chemical photoswitches. ACS Chem. Neurosci. *5*, 895–901.
50. Flannery, J.G., and Greenberg, K.P. (2006). Looking within for vision. Neuron *50*, 1–3.
51. Greenberg, K.P., Pham, A., and Werblin, F.S. (2011). Differential targeting of optical neuromodulators to ganglion cell soma and dendrites allows dynamic control of center-surround antagonism. Neuron *69*, 713–720.
52. Wu, C., Ivanova, E., Zhang, Y., and Pan, Z.-H. (2013). rAAV-mediated subcellular targeting of optogenetic tools in retinal ganglion cells in vivo. PLoS ONE *8*, e66332.
53. Dalkara, D., Byrne, L.C., Klimczak, R.R., Visel, M., Yin, L., Merigan, W.H., Flannery, J.G., and Schaffer, D.V. (2013). In vivo-directed evolution of a new adeno-associated virus for therapeutic outer retinal gene delivery from the vitreous. Sci. Transl. Med. *5*, 189ra76.
54. Petrs-Silva, H., Dinculescu, A., Li, Q., Min, S.H., Chiodo, V., Pang, J.J., Zhong, L., Zolotukhin, S., Srivastava, A., Lewin, A.S., and Hauswirth, W.W. (2009). High-efficiency transduction of the mouse retina by tyrosine-mutant AAV serotype vectors. Mol. Ther. *17*, 463–471.

OMTM, Volume *18*

Supplemental Information

Comparison of AAV-Mediated Optogenetic Vision Restoration between Retinal Ganglion Cell Expression and ON Bipolar Cell Targeting

Qi Lu, Tushar H. Ganjawala, Andrea Krstevski, Gary W. Abrams, and Zhuo-Hua Pan

SUPPLEMENTARY MATERIAL

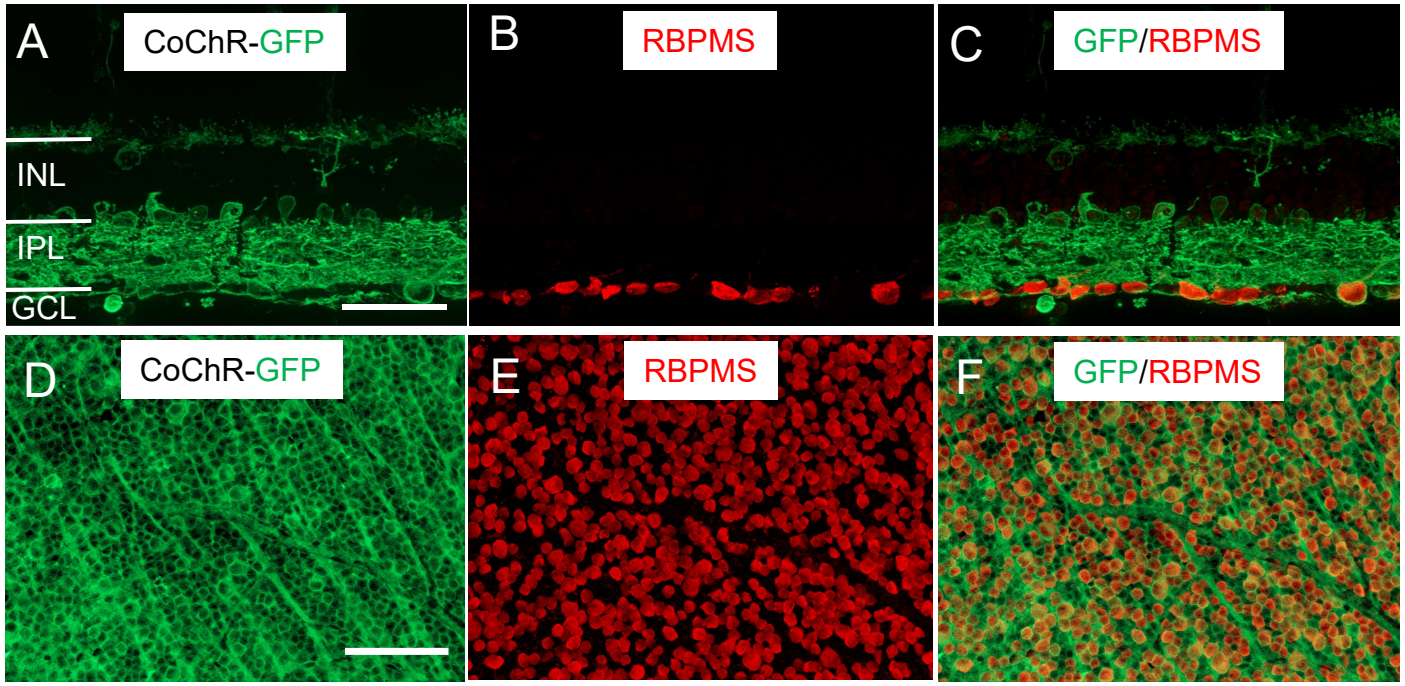

Figure S1. Expression of CoChR-GFP following ubiquitous RGC expression
Representative immunofluorescence images show the co-labeling of GFP (green) and RBPMS (red) in retinal vertical sections (A–C) and retinal whole mounts (D–F). RBPMS is an RGC-specific marker. GFP expression was observed in the vast majority of RGCs, many amacrine cells, and some horizontal cells, as evidenced in retinal vertical sections (C). The vast majority of RGCs were transduced by virus vectors based on the co-labeling of GFP and RBPMS in retinal whole mounts (F). The images of retinal whole mounts were captured with the focal plane in the retinal ganglion cell layer. Scale bars, 50 μm (A–C) and 100 μm (D–F).